NRC·CNRC

NRC Publications Archive
Archives des publications du CNRC

PVT properties of linear and dendritic polymers

Utracki, Leszek; Simha, Robert

This publication could be one of several versions: author's original, accepted manuscript or the publisher's version. / La version de cette publication peut être l'une des suivantes : la version prépublication de l'auteur, la version acceptée du manuscrit ou la version de l'éditeur.
For the publisher's version, please access the DOI link below./ Pour consulter la version de l'éditeur, utilisez le lien DOI ci-dessous.

Publisher's version / Version de l'éditeur:
https://doi.org/10.1002/polb.21893
Journal of Polymer Science Part B: Polymer Physics, 48, 3, pp. 322-332, 2009-12-22

NRC Publications Record / Notice d'Archives des publications de CNRC:
https://nrc-publications.canada.ca/eng/view/object/?id=5930e7ab-3c0a-4936-ab0f-ff785795f5a0
https://publications-cnrc.canada.ca/fra/voir/objet/?id=5930e7ab-3c0a-4936-ab0f-ff785795f5a0

Access and use of this website and the material on it are subject to the Terms and Conditions set forth at https://nrc-publications.canada.ca/eng/copyright
READ THESE TERMS AND CONDITIONS CAREFULLY BEFORE USING THIS WEBSITE.

L'accès à ce site Web et l'utilisation de son contenu sont assujettis aux conditions présentées dans le site https://publications-cnrc.canada.ca/fra/droits
LISEZ CES CONDITIONS ATTENTIVEMENT AVANT D'UTILISER CE SITE WEB.

Questions? Contact the NRC Publications Archive team at PublicationsArchive-ArchivesPublications@nrc-cnrc.gc.ca. If you wish to email the authors directly, please see the first page of the publication for their contact information.

Vous avez des questions? Nous pouvons vous aider. Pour communiquer directement avec un auteur, consultez la première page de la revue dans laquelle son article a été publié afin de trouver ses coordonnées. Si vous n'arrivez pas à les repérer, communiquez avec nous à PublicationsArchive-ArchivesPublications@nrc-cnrc.gc.ca.

National Research Council Canada | Conseil national de recherches Canada

Canada

PVT Properties of Linear and Dendritic Polymers

ROBERT SIMHA,[†] LESZEK A. UTRACKI

National Research Council Canada, Industrial Materials Institute, 75 de Mortagne, Boucherville, Quebec, Canada J4B 6Y4

Received 31 July 2009; revised 15 October 2009; accepted 16 October 2009
DOI: 10.1002/polb.21893
Published online in Wiley InterScience (www.interscience.wiley.com).

ABSTRACT: The aim of this article is to examine the limits of applicability of the Simha-Somcynsky (S-S) equation of state (EOS) by comparing the pressure-volume-temperature (*PVT*) data and the derivatives (compressibility, κ, and thermal expansion coefficient, α) of anionic linear polystyrene (PS) with poly(benzyl ether) dendrimers (PBED). Fitting the *PVT* of PBED data to the S-S EOS was similarly satisfactory as that of PS and the computed Lennard-Jones (L-J) interaction parameters showed similar errors of ca. 1%. Next, the experimental derivatives, α and κ of PS and PBED were compared with these functions computed from the S-S EOS—good agreement was obtained for α at ambient pressure, *P*, indicating validity of the S-S theory at least up to the first derivative. While the predicted $\kappa = \kappa(P)$ dependence for PS and a linear PBED homologue was correct, for dendrimers the compressibility was higher at low pressure and it was lower at high *P* than theory predicts. Also the extracted values of the L-J repulsion volume, v^*, between a segment pair was smaller than expected. The specific architecture of dendrimer molecules is responsible for this behavior, since their 3D configuration is significantly different from the S-S model with uniform segmental density and oxygen bonds in the main and side chains add flexibility.
© 2009 NRC Canada. J Polym Sci Part B: Polym Phys 48: 322–332, 2010

KEYWORDS: compressibility; dendrimer; free volume; melt; polystyrene; PVT; thermal expansion coefficient; thermodynamics

INTRODUCTION The physical properties of macromolecules with different architecture are of considerable interest. Besides the linear polymers, those with 2D and 3D have been prepared. Their properties in bulk or in solution, and the differences between these and linear ones are of concern. Our aim in this article is analysis of the thermodynamics of poly(benzyl ether), PBE, and its dendrimers, PBED, and comparison with polystyrenes (PS).[1,2] Hay et al. studied several generations of PBE in the molten state, in particular the pressure-volume-temperature (*PVT*) relationships as well as the derivative properties, compressibility, κ (reciprocal of the bulk modulus *B*) and the thermal expansion coefficient, α:

$$\kappa \equiv -(\partial \ln V/\partial P)_T = \kappa(T,P) = 1/B$$
$$\alpha \equiv (\partial \ln V/\partial T)_P = \alpha(T,P) \quad (1)$$

Dendrimers are the most highly branched 3D, nonentangled macromolecules with the degree of polymerization (DP) increasing with the generation number, *i*, and the residual functionality, *f*. Because of the nonmonotonic change of segmental density with *i*, the physical properties (e.g., intrinsic viscosity, compressibility, free volume) are nonmonotonic, having local maxima at $i \approx 4$–5. Their DP and shape change with *f* and *i* starting from a central core unit: $\mathrm{DP} = 1 + \sum_{i=1}^{n} f^i$. PBED (see Fig. 1) has been prepared by the convergent growth method, starting with 3,5-di hydroxy benzyl alcohol, thus the residual functionality, $f = 2$. Upon addition of generations in a homologous series, the molecular architecture changes from initially extended to a globular, what results in nonlinear variation of physical and chemical properties, e.g., a plot of intrinsic viscosity versus generation number, *i*, shows a maximum at about G_4-G_5.[3] The major difference between the linear and dendritic polymers is that while the former entangles, the latter does not. Since dendrimers are nearly monodispersed, for the comparison anionic PS's with low polydispersity should be used.[4–6]

The Simha-Somcynsky (S-S) equation of state (EOS) and related properties of linear polymer melts, their solutions, blends, foams, and nanocomposites have been discussed in terms of a lattice-hole theory.[7–10] The theory has been quantitatively successful for the numerous molten polymers and their mixtures to which it has been applied.[11–17] The S-S lattice model assumes the presence of empty cells, or a hole fraction, $h = h(V, T)$. The quantity *h* is a particular measure of the free volume content and for the equilibrium melts it is obtained by minimization of the Helmholtz free energy. An extension of this approach to dendrimers may be problematic considering the nonlinear segmental density in a homologous series.

[†]Deceased.
Correspondence to: L. A. Utracki (E-mail: leszek.utracki@cnrc-nrc.gc.ca)
Journal of Polymer Science: Part B: Polymer Physics, Vol. 48, 322–332 (2010) © 2009 NRC Canada.

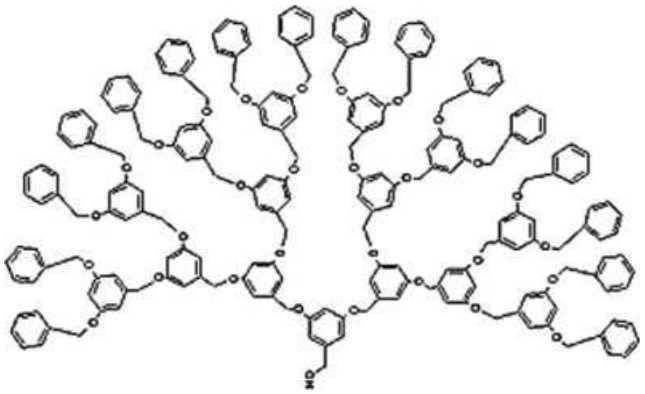

FIGURE 1 The fourth generation, G_4, of a poly(benzyl ether) dendrimer (PBED) with an —OH core and mers with residual functionality $f = 2$.

We propose here a modest aim—an analysis of the *PVT* behavior of PBED and PS series, trying to answer three questions:

1. To what extent can an "equivalent" linear system with the identical configurational thermodynamic properties as the dendrimer be conceived?
2. Can the characteristic segmental interaction parameters be extracted from the experimental *PVT* data by the means of the lattice-hole theory?
3. How the free volume and derivative properties change with the increasing generations?

THE SIMHA-SOMCYNSKY (S-S) THEORY

The S-S statistical thermodynamics theory leads to Helmholtz configurational free energy in reduced variables, $\tilde{F} = \tilde{F}\left[\tilde{V}, \tilde{T}, h(\tilde{V}, \tilde{T})\right]$, for small molecule liquids (e.g., benzene) or linear macromolecules—the magnitude of the external coordination number, $3c$, and the number of statistical segments per molecule, s, differentiate these two classes of liquids. The equation of state, EOS, is complex in form of coupled equations that need to be solved simultaneously. The first equation follows from the definition of equilibrium pressure, $\tilde{P} = -(\partial\tilde{F}/\partial\tilde{V})_{\tilde{T}}$, and the second from the minimization condition, $(\partial\tilde{F}/\partial h)_{\tilde{T},\tilde{V}} = 0$:[8,9]

$$\tilde{P}\tilde{V}/\tilde{T} = (1-\eta)^{-1} + 2yQ^2\left(1.011Q^2 - 1.2045\right)/\tilde{T} \qquad (2)$$

$$3c\left[\left(\eta - \frac{1}{3}\right)/(1-\eta) - yQ^2\left(3.033Q^2 - 2.409\right)/6\tilde{T}\right] + (1-s) - \frac{s\ell n(1-y)}{y} = 0 \qquad (3)$$

with the following definitions: $y = 1 - h$ is the fraction of occupied lattice sites; $Q = 1/(y\tilde{V})$, $\eta = 2^{-1/6}\, yQ^{1/3}$; s is the number of statistical segments per chain of the number-averaged molecular mass $M_n = sM_s$, where the latter is the segmental mass; v^* is the Lennard-Jones (L-J) repulsion volume between a segment pairs; ε^* is the L-J attraction energy between a segment pair; $qz = s(z-2) + 2 = 10s + 2 \approx 10s$. For high molecular weight linear polymers eqs 2 and 3

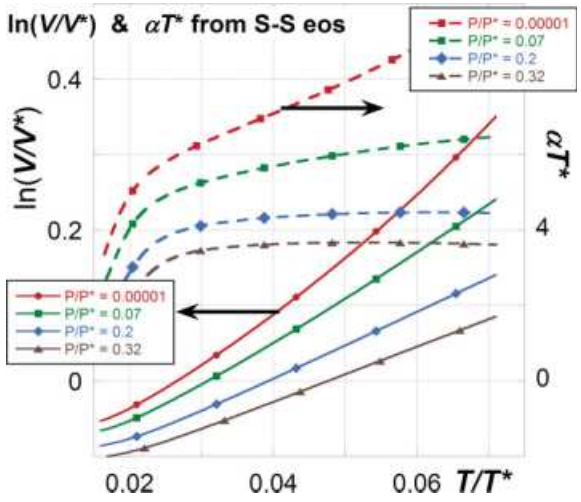

FIGURE 2 The reduced isobaric functions, lnV and α versus the reduced temperature, $\tilde{T} = T/T^*$, in the full potential range $T/100 = 1.6$–7.1. [Color figure can be viewed in the online issue, which is available at www.interscience.wiley.com.]

may be simplified assuming that $3c/s = 1 + 3/s \to 1$. The three characteristic scaling (material) parameters are defined as:

$$\left.\begin{array}{l} V^* = v^*/M_s; \\ P^* = zq\varepsilon^*/sv^*; \\ T^* = zq\varepsilon^*/Rc \end{array}\right\} \Rightarrow P^*V^*M_s/T^* \cong R/3 \qquad (4)$$

with $R = 8.314472$ (J/K mol) being the gas constant. Presently, these parameters are known for more than 60 polymers and they lead to an effective principle of corresponding states for molten polymers and their mixtures with gas, liquid or solid.

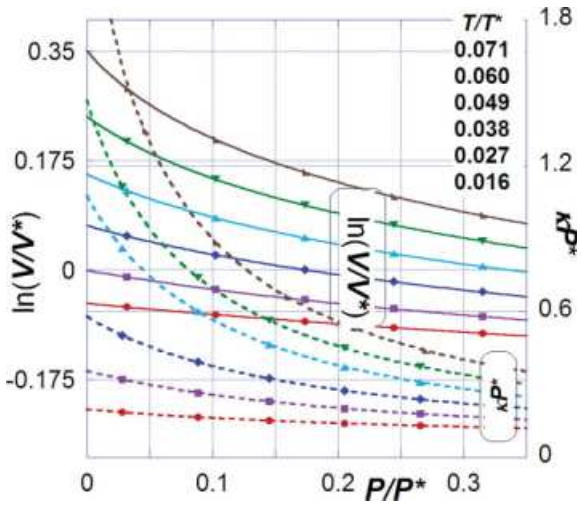

FIGURE 3 The reduced isothermal functions, lnV and κ, versus the reduced pressure, $\tilde{P} = P/P^*$, in the full potential range of $P = 10^{-5}$–0.32. [Color figure can be viewed in the online issue, which is available at www.interscience.wiley.com.]

TABLE 1 Statistics of S—S EOS fit to PVT Data for Zoller's PS Samples, Assuming $3c/s = 1$

Parameter	PS-09	PS-9	PS-34	PS-110
M_w (kDa)	0.91	9.54	34.5	110
M_w/M_n (−)	1.16	1.06	1.06	1.06
V (mL/g) at ambient	0.9747	0.9658	0.9628	0.9569
T_g (K)	288	362	371	374
Standard deviation, σ	0.001027	0.000565	0.000560	0.000975
R-squared, r^2	0.9999990	0.9999997	0.9999997	0.999999
Coefficient of determination, COD	0.999335	0.999640	0.999625	0.998997
P^* (bar)	8272 ± 48	7949 ± 31	8277 ± 34	8044 ± 45
T^* (K)	11062 ± 24	11707 ± 24	12029 ± 28	12256 ± 37
$10^4 \times V^*$ (mL/g)	9796 ± 5	9690 ± 5	9579 ± 5	9581 ± 7
M_s (g/mol)	37.83 ± 0.32	42.11 ± 0.29	42.05 ± 0.29	44.07 ± 0.41
ε^* (kJ/mol)	30.66 ± 0.07	32.45 ± 0.07	33.34 ± 0.08	33.99 ± 0.10
v^* (mL/mol)	37.06 ± 0.33	40.81 ± 0.30	40.28± 0.30	42.22 ± 0.43

For molten polymers, the full range of reduced independent variables is $P/P^* \equiv \tilde{P} = 10^{-5} - 0.32$ and $\tilde{T}/100 = 1.6 - 7.1$.[12] Within this space, the reduced volume and the eq 1 derivatives, computed from eqs 2 and 3, are displayed in Figures 2 and 3 as $\ln \tilde{V}$ and $\tilde{\alpha}$ versus $\tilde{T}$, and $\ln \tilde{V}$ and $\tilde{\kappa}$ versus $\tilde{P}$, respectively. The plots were generated by computing 300 values of $\ln \tilde{V}$ at constant $\tilde{P}$ or $\tilde{T}$, and then differentiating them by the Stineman normalization and differentiation method. The results illustrate that: (1) While $\ln \tilde{V}$ versus a reduced variable can be approximated by a second order polynomial with the correlation coefficient $r = 0.99999$, to fit with a similar precision the derivatives, α or κ, requires not the expected first order, but at least the 7th order polynomial. (2) The usefulness of a simple approximate expression is limited to a narrow range of independent variables.

During the 40 years that elapsed since publication of the S-S theory, the EOS was found to provide invariably precise fit to experimental *PVT* data for liquids, solutions, blends, foams, composites and nanocomposites. Since the theory is in reduced variables this agreements point out that all the tested systems studied so far follow the same $V = V(T, P)$ dependence, scaled by the L-J interaction parameters—the equilibrium liquids do follow the principle of corresponding states.

In spite of the precision and wide applicability of the S-S theory, it did not find as wide acceptance as it deserves. The reason rests in the algebraic complexity of the coupled eqs 2 and 3. As a partial solution several simplifying expressions of the S-S EOS have been suggested—some of these will be discussed in the following parts.[12,18–20]

SIMPLIFIED EXPRESSIONS

Simple expressions for V and/or its T or P derivatives are frequently of interest. As an early result in this direction, two expressions, valid in the limit of ambient-pressure, were proposed[18]:

$$\begin{aligned} &\ln \tilde{V} = a_o + a_1 \tilde{T}^{3/2} \\ &\tilde{\alpha} \equiv \left(\partial \ln \tilde{V}/\partial \tilde{T}\right)_P = (3a_1/2)\tilde{T}^{1/2} = 35.7810\tilde{T}^{1/2} \end{aligned} \tag{5}$$

where for $3c/s = 1$: $a_o = -0.10335$ and $a_1 = 23.8345$. Subsequently, formal expressions for isobaric α and isothermal κ were derived.[19] For $P \to 0$ the thermal expansion coefficient (with deviation from the exact solution by less than 1%) has the form:

$$\tilde{\alpha} \equiv \alpha T^* = 0.629 + 32.52\tilde{T}^{1/2}; \quad 2.3 \le 10^2\tilde{T} \le 5.2 \tag{6}$$

The expression for κ has not been evaluated except for some comparisons with various forms of the Tait empirical equation:

$$\begin{aligned} &\tilde{\kappa} \equiv \kappa P^* = C_T\left[\tilde{V}(0,\tilde{T})/\tilde{V}(\tilde{P},\tilde{T})\right]/(\tilde{P} + \tilde{B}_T); \\ &\tilde{B}_T \equiv -\tilde{V}_o C_T\left(\partial\tilde{P}/\partial\tilde{V}\right)_T - \tilde{P} \end{aligned} \tag{7}$$

where $C_T \approx 0.0894$ is the Tait "universal" constant.[20]

More recently, the S-S EOS was analyzed for molten polymers (also assuming $3c/s = 1$) within full range of independent variables: $\tilde{P} = 10^{-5} - 0.32$ and $\tilde{T}/100 = 1.6 - 7.1$ The data were fitted to several six-parameter analytical expressions out of which the following form was the best:[12]

$$\begin{aligned} &\ln \tilde{V} = a_o + a_1\tilde{T}^{3/2} + \tilde{P}\left[a_2 + \left(a_3 + a_4\tilde{P} + a_5\tilde{P}^2\right)\tilde{T}^2\right] \\ &\therefore \textit{for } \tilde{P} \to 0: \quad \ln \tilde{V} = \sum_{i=0}^{3} a_i\left(\tilde{T}^{3/2}\right)^i \end{aligned} \tag{8}$$

Table 1 of ref. 12 provides the a_i coefficients and the error statistics. The ambient pressure thermal expansion coefficient from eq 8 is:

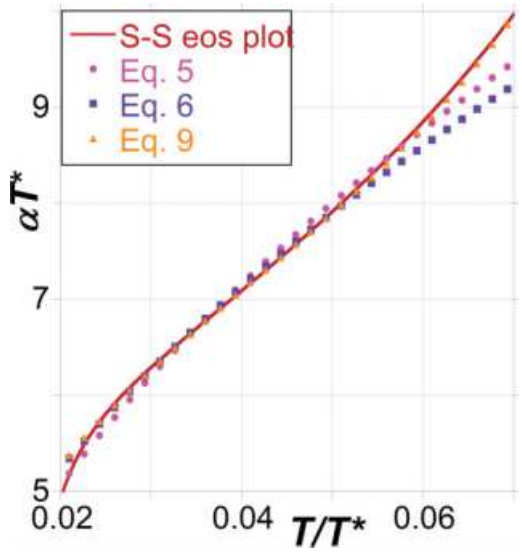

FIGURE 4 Comparison of the $\tilde{\alpha} = \alpha T^*$ versus $\tilde{T} = T/T*$ dependence predicted by eqs 2 and 3 with three approximate expressions. Size of the symbols corresponds to the computational error of about ±0.3%. [Color figure can be viewed in the online issue, which is available at www.interscience.wiley.com.]

$$\tilde{\alpha} = 38.9377\tilde{T}^{1/2} \times \left[1 - \left(18.1368\tilde{T}^{3/2} + 880.079\tilde{T}^{3}\right)\right] \quad (9)$$

For $\tilde{T} \to 0$ eq 9 reduces to the form of eq 5 with slightly larger coefficient. Figure 4 compares the exact $\tilde{\alpha}$-values at ambient pressure, $\tilde{P} = 10^{-5}$, computed from eqs 2 and 3, with those from the simplified expressions in eqs 5, 6, and 9. Apparently, eqs 5 and 6 offer reasonable approximations (error < 3%) within the range: $0.03 \le \tilde{T} \le 0.06$, but eq 9 is the best, following the theory with an error of <1% at $\tilde{T} > 0.023$.

Jain and Simha derived the compressibility expression as a function of the variables of state in terms of the Tait empirical expression.[19] However, the main question is if the S-S EOS correctly predicts κ for linear and dendritic macromolecules. This is easier answered computing directly the isobaric compressibility coefficient, $\tilde{\kappa}_T = \tilde{\kappa}(\tilde{P})$; of interest is mainly the low-pressure region, $\tilde{P} = 10^{-5} - 0.1$. Accordingly, the derivative was computed within this region from the S-S EOS at 11 levels of $\tilde{T}$ and 100 levels of $\tilde{P}$. The 1100 low-pressure data points were fitted to the second order polynomial:

$$\tilde{\kappa}_T = A_0 + A_1\tilde{P} + A_2\tilde{P}^2; \quad r \ge 0.999 \quad (10)$$

As evident from Figure 5, the temperature dependence of the A_i parameters is nearly exponential:

$$\begin{aligned} &A_i = c_{i1} \times exp\{c_{i2} \times \tilde{T}\}; \quad r_i; \quad i = 0 - 2 \\ &c_{01} = 0.110; \quad c_{11} = -0.189; \quad c_{21} = 0.333 \\ &c_{02} = 43.17; \quad c_{12} = 70.62; \quad c_{22} = 85.33 \\ &r_0 = 0.9989; \quad r_1 = 0.9992; \quad r_2 = 0.9996 \end{aligned} \quad (11)$$

The parameters A_i in eq 11 are exact and might be used to assess validity of an approximate expression computed from eq 8 (values of a_i taken from[12]):

$$\begin{aligned} &-\tilde{\kappa} = a_2 + a_3\tilde{T}^2 + 2a_4\tilde{T}^2\tilde{P} + 3a_5\tilde{T}^2\tilde{P}^2; \quad \text{thus :} \\ &A_0 = 0.132 + 333.7\tilde{T}^2; \quad A_1 = -2065\tilde{T}^2; \quad A_2 = 3990\tilde{T}^2 \end{aligned} \quad (12)$$

Figure 5 shows that agreement for A_i computed from EOS and calculated from eq 12 is reasonable only for A_0 and A_1 (10% error for $0.02 \le \tilde{T} \le 0.05$) while for A_2 it is acceptable at $\tilde{T} \approx 0.03$. It is noteworthy that while α is the first derivative of V, A_1 is the second and A_2 is the third one, thus for these larger errors are expected.

Instead of the compressibility coefficient, Hay et al.[1] considered the pressure dependence of the compression modulus $B = -v(\partial P/\partial v)_T = 1/\kappa$ in the expanded form:

$$B = \tilde{B}P^* = B_o + B_1P + B_2P^2 \quad (13)$$

From eqs 10 and 13 the between B and κ coefficients are:

$$\begin{aligned} &\tilde{B} = 1/\tilde{\kappa} = (1/A_o)\left(1 - A_1\tilde{P}/A_o - A_2\tilde{P}^2/A_o\right) \quad \text{thus :} \\ &\tilde{B} = B/P^* = \left[B_o + B_1P + B_1P^2\right]/P^* \\ &B_o = P^*/A_o; \quad B_1 = -A_1/A_o^2; \quad B_2 = -A_2/A_o^2P^* \end{aligned} \quad (14)$$

In the latter part we shall compare the experimental B_i-values[1] with those predicted by S-S EOS, as well as calculated through A_i given by eq 12.

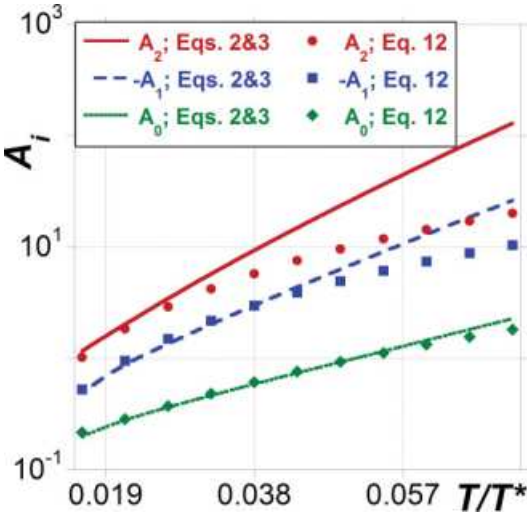

FIGURE 5 Temperature dependence of $\tilde{\kappa}$ versus $\tilde{P}$ coefficients in eqs 10–12 versus $\tilde{T} = T/T^*$. Solid lines are computed from S-S EOS, while points are from eq 12. [Color figure can be viewed in the online issue, which is available at www.interscience. wiley.com.]

TABLE 2 Statistics of S—S EOS Fit to *PVT* Data for PBED Macromolecules

Parameters	G_3	G_4	G_5	G_6	$G_{5\text{-linear}}$
$M_w \approx M_n$ (kDa)	1.592	3.288	6.687	13.464	6.687
V (mL/g); 140 °C, P = ambient	0.8707	0.8516	0.8412	0.8691	0.8537
T_g (K)	307	314	317	318	321
Standard deviation, σ	0.0002928	0.0002442	0.0002392	0.0003423	0.0004043
Correlation coefficient sq., r^2	0.9999999	0.9999999	0.9999999	0.9999998	0.9999998
Coefficient of determination	0.9996759	0.9996267	0.9995466	0.9994128	0.9986771
P^* (bar)	12087 ± 22	13014 ± 64	12085 ± 56	12779 ± 28	12053 ± 180
T^* (K)	11303 ± 10	10726 ± 25	11567 ± 27	11971 ± 14	12736 ± 132
$10^4 \times V^*$ (mL/g)	8387 ± 2	8189 ± 5	8217 ± 4	8469 ± 2	8410 ± 15
M_s (g/mol)	30.90 ± 0.09	27.89 ± 0.22	32.28 ± 0.24	30.65 ± 0.24	34.82 ± 0.94
ε^* (Kj/mol)	31.33 ± 0.03	29.73 ± 0.07	32.06 ± 0.07	33.18 ± 0.04	35.30 ± 0.36
v^* (mL/mol)	25.92 ± 0.08	24.35 ± 0.21	26.52 ± 0.21	25.96 ± 0.22	29.28 ± 0.85

FITTING THE S-S EOS TO PS AND PBED EXPERIMENTAL DATA

We begin with the evaluation of the scaling parameters of Zoller and Walsh[4] data for the narrow molecular mass distribution, anionic PS samples discussed by Hay et al.[1] These polymers have already been fitted to the S-S EOS using several assumptions affecting numerical values of the scaling parameters.[5,6] However, for the present purpose the *PVT* data of PS will be fitted to S-S EOS assuming $3c/s = 1$. This assumption is reasonable for PS-110 where the weight-average molecular weight is $M_w = 110$ kDa, thus $3c/s = 1 + 3/s \approx 1.001$, but questionable for PS-09 with $M_w = 0.91$ kDa, thus $3c/s = 1.125$. As described before,[12–17] the *PVT* data were computer-fitted to eqs 2 and 3 using the MicroMath least squares optimization protocol. The initial values of the three scaling parameters were computed from eq 8. Table 1 lists the characteristics of the PS samples, the three statistical fitting parameters (σ, r^2 and COD), and the three scaling parameters (P^*, T^*, and V^*). Also shown is M_s (consistent with $3c/s = 1$) and the L-J interaction parameters from eq 4, ε^* and v^*. It is noteworthy that these results were obtained by a simultaneous, nonlinear, iterative fitting of the *PVT* data to eqs 2 and 3.

The small decrease of V^* with increasing molar mass mirrors the corresponding trend in specific volume seen in the third row of Table 1. It is reversed for the segmental molar mass, M_s, as more flexible, longer chains better pack into lattice. Overall, the effective segmental molar mass amounts to about 40% of the repeating unit [M(styrene) = 104.15 g/mol]. From eq 4 the molar activation energy, ε^*, is proportional to T^*, thus increasing with increasing molar mass, parallel to $v^* = V^* M_s$.

C. Hawker (IBM Research Division) synthesized the four dendrimers and their linear analogue, G. Hay (University of Queensland) studied their *PVT* behavior and M. E. Mackay sent us tabulated data.[1,2] These were fitted to S-S EOS using the same nonlinear optimization program as that used for PS. Table 2 lists the corresponding information. The experimental volume at ambient pressure exhibits a minimum for G_5 and that of the linear analogue, $G_{5\text{-linear}}$, is slightly larger.[1] These features are reproduced in the calculations of the equivalent system. The specific repulsion volume, v^*, assumes a minimum at G_4, while the ambient pressure specific volume, V_o, shows minimum for G_5. The same obtains in respect to T^*, thus ε^*. Behavior of P^* is more complex, influenced by both ε^* and v^*. In the G-series, there is a dual influence of the molecular architecture and the molar mass. For example, for the odd-numbered generations P^* is nearly constant, $P^* = 1.2075 \pm 0.0011$, smaller than that obtained for the even-number ones $P^* = 1.2897 \pm 0.0121$ GPa. As discussed later, there are also other effects of the molecular architecture.

Summing up, the data in Tables 1 and 2 indicates that the S-S EOS fits the experimental data for PS and PBED with similar precision, *viz*. the standard deviation, the correlation coefficient squared and the coefficient of determination are all comparable. It seems that modeling dendromeric $V = V(T, P)$ function as that of a mean-averaged linear macromolecular chain with $3c/s = 1$ is acceptable. It is noteworthy that the worst fit of the five PBE is that of linear $G_{5\text{-linear}}$. Thus, the S-S EOS can be used for describing the dendrimers' *PVT* surface. However, are the values of the extracted interaction parameters and derivative properties acceptable?

INTERACTION PARAMETERS AND FREE VOLUME OF PS AND PBED

Computed values of the L-J binary interaction parameters, ε^* and v^*, represent the intersegmental interactions, which for linear polymers increase with molecular weight, viz. ε^*, $v^* = a_0 + a_1 \log (M_w)$.[5] Formally, for a given family of polymers with different M_w with $P^* \propto$ CED being relatively constant, the L-J parameters are interrelated, viz.: $\varepsilon^* \simeq v^* P^*/10$.[13] However, empirically a linear dependence between the two L-J parameters is usually is found.[5,14,21] Simha[22] derived the following dependence:

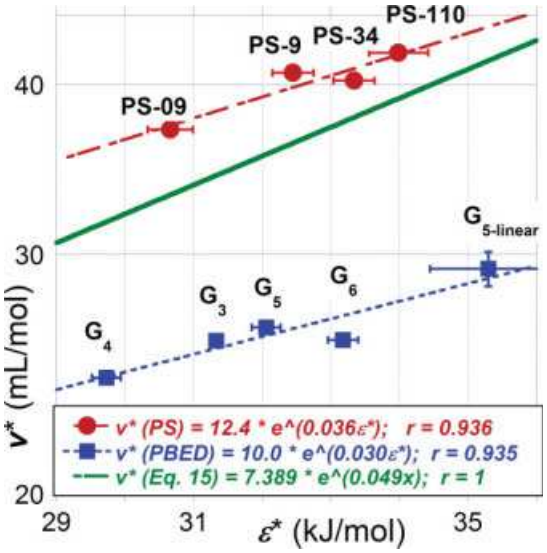

FIGURE 6 Correlation of the L-J interaction parameters, v^* versus ε^*, for PS and PBE. The solid line follows eq 15. [Color figure can be viewed in the online issue, which is available at www.interscience.wiley.com.]

$$T^* = 10^4 \ln(M_s v^*/A)^x \Rightarrow \ln v^* \simeq 2 + \varepsilon^*/2 \qquad (15)$$

Figure 6 displays the v^* versus ε^* relationships for PS, PBED and that predicted by eq 15. Excepting data for $G_{5\text{-linear}}$ a similar scatter of data points is apparent for both series of polymers. Surprisingly, while for PS the sequence of data points depends on log (M_w), for PBED it does not—the smallest values of v^* and ε^* are observed for G_4 and the largest for $G_{5\text{-linear}}$. In other words, plotting v^* or ε^* versus M_w for the dendrimer series would show a local minimum for G_4, maximum for $G_{5\text{-linear}}$ with small changes of value for G_5 and G_6.

Characteristically, for the same range of $\varepsilon^* = 29$–36 the repulsion volume, v^*, for PBED is smaller than that of PS by about 35%. Considering that the PBE data for dendrimers and linear molecules follow a similar dependence, the difference seems related mainly to chemical character of the two polymers that results in different backbone rigidity. In PS the C—C backbone is stiffened by the benzene ring attached to every second carbon atom, whereas in PBED series the ether linkages provides greater flexibility.[23] These differences translate into larger values of P^* for PBED than that for PS and thus larger CED. Significantly, judging by v^*-values of G_5 and $G_{5\text{-linear}}$, the effect of the macromolecular architecture is relatively small. We also note low statistical certainty of the scaling parameters for $G_{5\text{-linear}}$, but even these cannot hide the large differences of the repulsion volume, v^*, between PS and PBED.

Next, we examine the relations between the hole fraction, h, and M_w at T = 400 K and at two pressures of $P = 20$ and 140 MPa (see Fig. 7). For linear PS h increases with log (M_w), but for PBED the free volume reaches maximum at G_4, where the L-J interaction parameters are at minimum. Note that at the limit $\tilde{P} \to 0$ an approximate solution of eq 3 gives:[22]

$$h \simeq 1 - 0.957/\tilde{V} \qquad (16)$$

The ranking of h by this relation follows the PS-dependence in Figure 7. The "equivalent" model reproduced the property extrema observed near G_4 or G_5. The free volume content, h, in $G_{5\text{-linear}}$ is smaller than that in G_5. At $P = 140$ MPa h-value "coincidently" falls on the PS dependence. However, since in Tables 1 and 2 the magnitude of P^* is significantly different for PS than for $G_{5\text{-linear}}$ the "coincidence" will not be observed at other pressures.

DERIVATIVES OF PS AND PBED: α AND κ

In this Part, we examine capability of the S-S EOS of predicting the magnitudes of the two principal derivatives, α and κ. The discussion is in two parts, the first focusing on the direct comparison of S-S EOS theoretical results with the experimental data and the second on the usefulness of simplified relations for the same purpose.

As Tables 1 and 2 shows, S-S EOS well describes the *PVT* data. To find out whether the agreement extends to derivatives one needs to compare results of differentiation of computed and experimental functions of $\ln V = f(T)$ or $f(P)$. Table 3 lists results of these calculations for the thermal expansion coefficient of G_3 and G_6. The T-independent values of α have well-acceptable mean-average difference, $\mathrm{MAD}(f) \equiv 100 \sum_{i=1}^{N} \mathrm{ABS}\,(f_{\mathrm{exp},i}/f_{\mathrm{calc},i} - 1)/N$, between the experimental and computed from the S-S EOS α-values, viz.: $\mathrm{MAD}_{G3}(\alpha) = 0.35\%$ and $\mathrm{MAD}_{G6}(\alpha) = 0.61\%$.

Next the compressibility coefficient of G_6 was calculated as $\kappa(G_6) = \kappa(P)$. For the specific volume, the mean difference between the experimental and computed values is $\mathrm{MAD}_{G6}(\ln V) = 0.13\%$, while that of the compressibility coefficient is $\mathrm{MAD}_{G6}(\kappa) = 1.7\%$—in face value both quite acceptable. However, as shown in Figure 8, $\kappa(G_6)$ deviated systematically; at low P, the experimental values are larger than S-S EOS predictions, while at high P they are lower. To test whether the error originates in inadequacy of the theory or dendrimers' molecular architecture, the computation was repeated for PS-110. In this case, the mean difference between the experimental and computed values of $\ln V$ was $\mathrm{MAD}_{PS110}(\ln V) = 0.08\%$, and that of κ is $\mathrm{MAD}_{PS110}(\kappa) = 1.2\%$. Furthermore, for PS-110 (see Fig. 9) the error is random, although at the highest T it seems to increase with P.

Similar computations were also performed for the remaining members of the PBED family. The analysis might be summarized as:

1. For linear polymers and low generation number dendrimers (such as G_3) the S-S EOS provides excellent description of the primary function, $V = V(P, T)$ and a good one for the first derivatives, e.g., α_o and $\kappa_o = \kappa(P = 0)$. It is the second derivative, e.g., $(\partial\kappa/\partial P)_T = (\partial^2 \ln V/\partial P^2)_T$ that leads to a random error about one order of magnitude larger than that of V or α.
2. For dendrimers G_4, G_5, and G_6 there is a systematic difference between the experimental and predicted compressibility gradient, $(\partial\kappa/\partial P)_T$—at low P it is easier to compress dendrimers than the linear, entangled polymers,

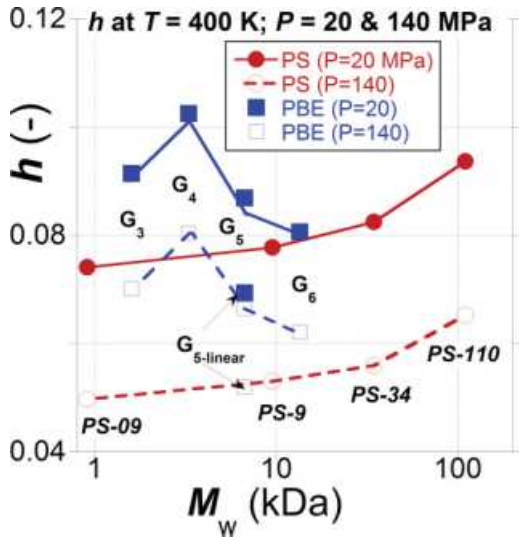

FIGURE 7 Hole fraction for the equivalent chains of PS and PBE versus molecular weight at $T = 400$ K and $P = 20$ and 140 MPa.

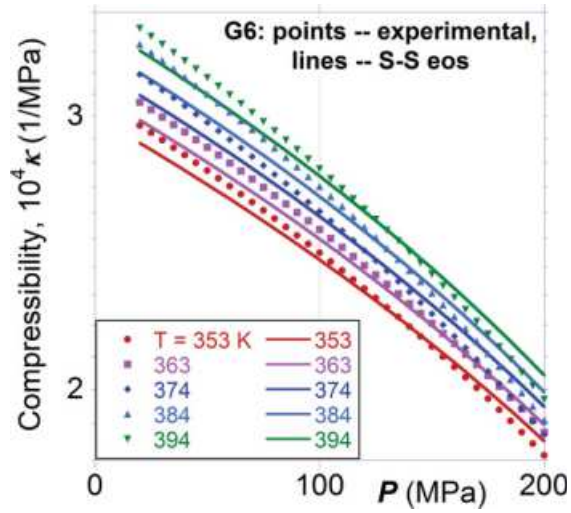

FIGURE 8 Compressibility coefficient versus pressure at five temperatures for G_6. Points are experimental, lines were computed from eqs 2 and 3.

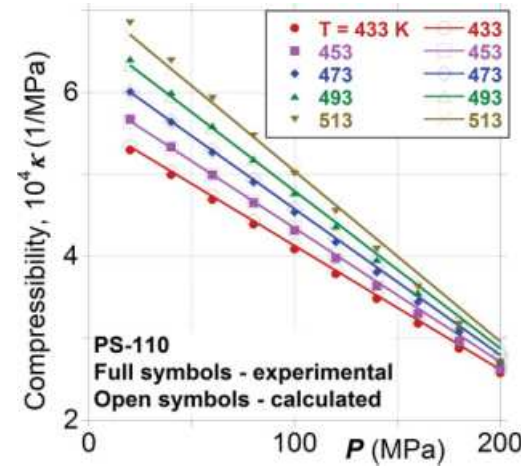

FIGURE 9 Compressibility coefficient versus pressure at five temperatures for PS-110. Solid points are experimental, open points and lines were computed from eqs 2 and 3.

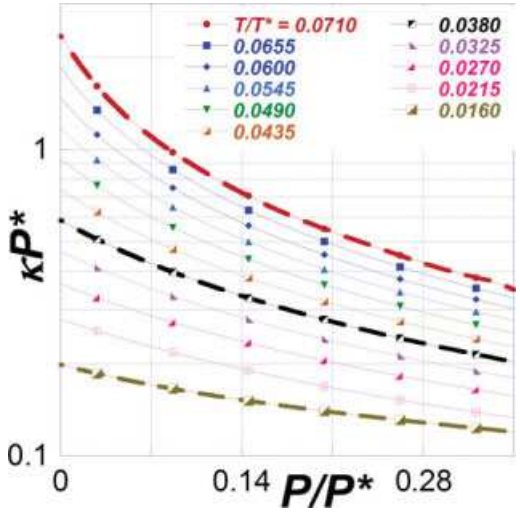

FIGURE 10 Computed from eqs 2 and 3 reduced dependence, κ versus P, in full range of independent variables. The three broken lines are the 7th order polynomials fitted to the data with $r \geq 0.99999$.

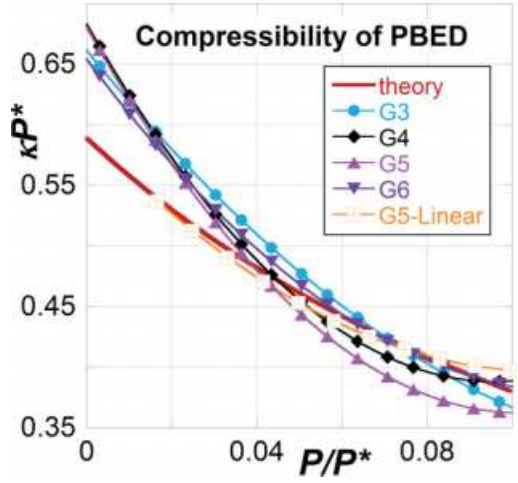

FIGURE 11 Reduced compressibility versus reduced pressure for PBE. Points computed from the S-S EOS values for the G-series and $G_{5\text{-linear}}$; solid line predicted values by S-S EOS.

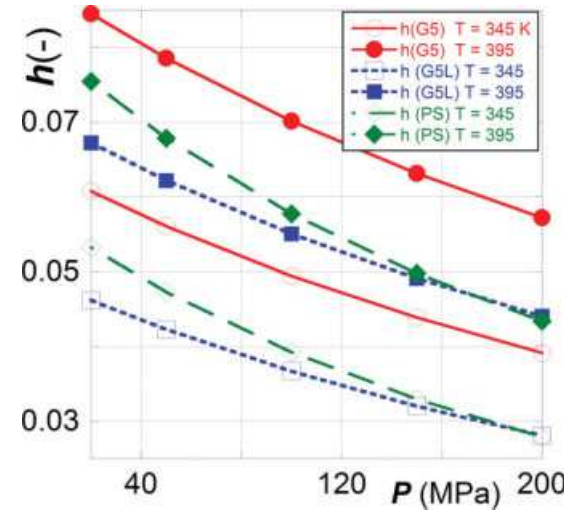

FIGURE 12 Free volume parameter h versus P at $T = 345$ and 395 K for dendrimer G_5, its linear analogue, $G_{5\text{-linear}}$ and PS-34.

TABLE 3 Experimental and Predicted by the S-S EOS Values of the Thermal Expansion Coefficient for Dendrimers G_3 and G_6

P (MPa)	$10^4\alpha(G_3)$ exp.	$10^4\alpha(G_3)$ calc.	$10^4\alpha(G_6)$ exp.	$10^4\alpha(G_6)$ calc.
0	–	5.849	–	5.365
20	5.578	5.567	5.095	5.100
40	5.311	5.310	4.876	4.886
60	5.066	5.080	4.708	4.694
80	4.854	4.874	4.546	4.519
100	4.678	4.688	4.398	4.361
120	4.524	4.519	4.276	4.215
140	4.374	4.364	4.121	4.089
160	4.245	4.222	3.958	3.956
180	4.116	4.091	3.771	3.804
200	4.005	3.969	3.594	3.632

The mean-average difference between experimental and computed values of $\alpha(G_3)$ in the whole range of P is 0.35% and that of $\alpha(G_6)$ is 0.61%.

whereas at high P it is more difficult. This behavior indicates that the full applicability of the S-S EOS to this type of macromolecules does not extend to the level of second derivatives.

Next, we turn to derivatives calculable from the simplified expressions. The first numerical column of Table 4 list the experimental thermal expansivity coefficient[1,2] at ambient pressure and $T = 413$ K, α_o, to be compared with those computed from eqs 9 and 6. For PS, α_o regularly decreases with increasing M_w–the tendency well reproduced by the computed values.[5] The mean average difference between the experimental data and those estimated by eqs 9 and 6 are listed in the last two rows of Table 4 separately for PS and PBE. Evidently, eq 9 very well approximates α_o of linear polymers, but not so of dendrimers. The values computed from the simple eqs 5 or 6 approximate the experimental α_o-values of PS and PBE with a similar accuracy. For the PBE the plot of ambient pressure α_o resembles that of h in Figure 7. Plotting α_o versus M_w shows that the overall tendency for PS and PBED is similar—a decrease with increasing M_w. However, G_4 and $G_{5\text{-linear}}$ do not follow this dependence; their experimental and computed α_o-values are too high and too low, respectively.

Hay et al.[1] did not calculate the compressibility, but rather its reciprocal bulk modulus, $B = 1/\kappa = B_o + B_1P$. Thus, Table 4 compares the experimental values of B_o and B_1 coefficients cited by these authors with the results of eqs 10–14. The last two rows list the mean-average differences, MAD, between the experimental and predicted values of B_o and B_1. Generally, eq 11 performs slightly better than eq 12—B_o approximation with MAD of 7–11% is acceptable, but that of B_1 is less successful: 22–31% for PS and 117–130% for PBE. The source of this large difference is, on the one hand, wrong assumption that the bulk modulus is a linear function of pressure (e.g., see Fig. 10), and on the other the mentioned earlier different compressibility of dendrimers at low and high pressure as compared to linear polymers.

Numerical differentiation of $\ln V$ (computed from eqs 2 and 3) leads to $\tilde{\kappa} = \tilde{\kappa}(\tilde{P}, \tilde{T})$ displayed in Figure 10 within the full range of reduced variables.[12] Only the 7th order polynomial approximates the dependence with acceptable $r \geq 0.99999$. However, to check whether a low-level polynomial is applicable at low pressures, viz. $\tilde{P} \leq 0.1$, we examine the second order polynomial based on eqs 10–12. The procedure was as follows: First, the isothermal κ_T versus P data were fitted to the second order polynomials:

$$\begin{aligned} &\kappa_T = \sum_{i=0}^{2} a_i P^i; \quad \text{where} \\ &a_0 = A_0/P^*; \quad a_1 = A_1/P^* 2; \quad a_2 = A_2/P^* 3 \\ &a_i = c_{i1}\exp\{c_{i2}T\} \Rightarrow A_i = P^*(i+1)c_{i1}\exp\left\{T_i^* c_{i2}\tilde{T}\right\} \end{aligned} \tag{17}$$

Next, the a_i coefficients were plotted versus T and fitted to exponentials converting the a_i to A_i coefficients. Finally, the

TABLE 4 Experimental[a] and Calculated Derivatives at $T = 413$ K and $P = 0.10132$ Mpa

	$10^4\ \alpha_o$ (1/K)			B_o (1/GPa)			B_1		
Polymer	Exp[a]	Eq. 9	Eq. 6	Exp[a]	Eq. 11	Eq. 12	Exp.[a]	Eq. 11	Eq. 12
PS-9	5.746 ± 0.118	5.738	5.781	1.55	1.58	1.39	10.9	9.02	8.07
PS-34	5.524 ± 0.123	5.519	5.664	1.57	1.71	1.45	11.1	9.15	8.58
PS-110	5.367 ± 0.180	5.368	5.606	1.52	1.71	1.58	11.4	9.24	8.82
G_3	5.813 ± 0.162	6.033	5.713	1.98	2.27	1.58	20.3	8.84	8.99
G_4	6.149 ± 0.199	6.505	6.164	2.06	2.24	2.09	19.6	8.57	8.27
G_5	5.528 ± 0.087	5.837	5.524	2.22	2.35	2.08	18.0	8.96	7.79
G_6	5.372 ± 0.189	5.558	5.256	2.14	2.62	2.17	22.2	9.13	8.47
$G_{5\text{-Linear}}$	5.331 ± 0.286	5.088	4.805	2.31	2.70	2.41	17.3	9.42	8.78
MAD(PS) %	–	0.08	2.45	–	7.06	7.86	–	21.8	31.2
MAD(PBE) %	–	4.51	3.04	–	11.8	7.80	–	117	130

[a] The experimental values were taken from ref. 1.

TABLE 5 Calculation of Eq 17 coefficients at $T = 413$ K and $P = 0.101$ Mpa

	a_0			a_1			a_2		
POLYMER	c_{01}	$10^3 c_{02}$	r	$-c_{11}$	$10^3 c_{12}$	r	c_{21}	$10^3 c_{22}$	r
PS-9	0.1107	4.227	0.997	0.1930	7.010	0.987	0.1430	9.752	0.988
PS-34	0.0989	4.471	0.999	0.1123	8.168	0.996	0.0592	11.616	0.982
PS-110	0.1061	4.311	0.996	0.1830	7.120	0.984	0.2330	8.715	0.969
G_3	0.1266	3.408	0.971	0.6919	3.405	0.738	3.3742	2.015	0.370
G_4	0.1494	3.083	0.958	0.7167	3.984	0.644	1.3038	5.923	0.540
G_5	0.1516	2.985	0.999	0.6818	4.175	0.975	2.1218	4.778	0.967
G_6	0.1602	2.554	0.809	0.9239	2.508	0.332	1.3475	4.335	0.312
$G_{5\text{-linear}}$	0.1510	2.570	0.990	0.5036	3.740	0.966	0.0100	16.986	0.989

compressibility dependence (in reduced variables) was computed as $\tilde{\kappa} = \tilde{\kappa}(\tilde{P}, \tilde{T})$ at $\tilde{T} = 0.038$ and $0.0001 \leq \tilde{P} \leq 0.1$, using the scaling parameters from Tables 1 and 2, as well as the eq 17 parameters from Table 5.

The computation indicates that within the narrow range of P the second order polynomial in eq 17 provides acceptable level of accuracy, as compared with the complete theoretical prediction (within the full range of the independent variables the approximated values deviated less than 9% from the theory). Figure 11 displays the results for PBED with the theoretical prediction for reference. There is good agreement between the theory and experiment only for the linear PBE, $G_{5\text{-linear}}$, while the four PBED dendrimers strongly deviate from the theoretical curve; at low pressure they are more compressible than theoretically predicted, whereas at high pressure they are less. This behavior is especially large for G_4 and G_5.

DISCUSSION

The S-S theory has its roots in the Prigogine's cell theory of liquids with its square well potential and the corresponding states principle (CSP). To that crystal-like structure, Simha and Somcynsky introduced an optimum level of disorder as empty cells or holes, h, which increase the system entropy.[24] The theory describes the equilibrium thermodynamic behavior specifically of chain and monomeric, spherical molecules, the latter particularly suitable for testing the CSP. Thus, this mean-field theory assumes presence of randomly placed, interconnected statistical segments in the partially filled lattice. The free volume dependence on the number of empty cells is an additive function of the "solid-like" and "gas-like" modes of segmental motion. The configuration of the molecules is characterized by two structural parameters, s and $3c$. Furthermore, as it can be deduced from eq 3, CSP requires that s is large and the ratio $3c/s$ universal.[7,8] In consequence, when comparing a polymer PVT behavior with the S-S EOS the assumptions $3c/s = 1$ is most logical. Utracki[5] showed that allowing $3c/s$ to adopt other values may improve the fit, but it leads to unrealistic values of this structural quantity.

The aim of this article is not an analysis of the PVT behavior of PBED *per se*, but rather an analysis how much an "equivalent" mean-field model is capable predicting the observed behavior, or more specifically, the article attempts answering the three basic questions posed in Introduction. Thus, yet again we test the limits of applicability of the S-S theory, originally developed for a single component at the thermodynamic equilibrium (*viz*. polymer melts, solvents, solutions or miscible blends). Over the years, its applicability was extended to immiscible binary or ternary systems containing solid, liquid or gaseous dispersed phase.[24–28] However, in all these cases the matrix was composed of linear, entangled polymers, which dominated the thermodynamic behavior. By contrast, dendrimers constitute a new class of nonentangled macromolecules with nonuniform segmental density, which changes with the generation number. Application of the S-S EOS implies that these macromolecules are treated as "equivalent" linear system with the "equivalent" configurational thermodynamic properties.

Re Question 1

To what extent can an "equivalent" linear system with the identical configurational thermodynamic properties as the dendrimer be conceived?

Comparison of data in Tables 1 and 2 shows that the S-S model provides as good fit to the PVT data of poly(benzyl ethers), PBE, as that of PS. Even in the worst case of $G_{5\text{-Linear}}$, the three statistical fit parameters are similar to these of PS-110.

In short, eqs 2 and 3 (with $3c/s = 1$) describe the $V = V(T, P)$ surface of dendrimers as well as that of linear chain macromolecules. Furthermore, good predictability of the EOS extends to first derivatives, such as α_o and κ_o, but the agreement breaks down for higher derivatives. In contrast with the S-S theory and behavior of linear polymers, the dendrimers' compressibility is higher than expected at low and lower at high P. This behavior originates in the core-shell distribution of segmental density, documented by other measurements.[2,3]

Re Question 2

Can the characteristic segmental interaction parameters be extracted from the experimental PVT data by the means of the lattice-hole theory?

The L-J parameters, v^* and ε^*, depend not only on the chemical nature of the polymer, but also on the molecular

TABLE 6 Temperature Dependence of the Isobaric Free Volume Parameter, h, for G_5, $G_{5\text{-linear}}$ and PS-34

	G_5			$G_{5\text{-linear}}$			PS-34		
P (MPa)	$-10^2 h_o$	$10^4 h_1$	r (−)	$-10^2 h_o$	$10^4 h_1$	r (−)	$-10^2 h_o$	$10^4 h_1$	r (−)
20	10.306	4.7472	0.99999	9.9010	4.2070	0.99999	10.022	4.4459	0.99999
50	9.8929	4.4924	0.99999	9.5282	3.9856	0.99999	9.4963	4.1212	0.99999
100	9.3456	4.1410	0.99999	9.0135	3.6745	0.99999	8.8299	3.6960	0.99999
150	8.9125	3.8542	0.99999	8.5874	3.4156	0.99998	8.3134	3.3641	0.99999
200	8.5526	3.6130	0.99999	8.2194	3.1942	0.99998	7.8830	3.0928	0.99998

configuration and mass. As shown in Figure 6, the dependence of v^* versus ε^* for PBED is similarly linear as that for PS and eq 15. It is noteworthy that data for dendritic and linear PBE fall on the same line, thus the difference between PS and PBE is not related to the molecular architecture.

For low molecular weight paraffins as well as for polymer melts Simha and his collaborators reported linear correlation between v^* and the van der Waals hard core volume, V_w.[29,30] From the segmental molar volumes[31] we arrived at V_w, = 62.8 and 61.5 for PS and PBED, respectively. Evidently, the ratio V_w(PBED)/V_w(PS) = 0.98, is not comparable with v^*(PBED)/v^*(PS) = 0.67 ± 0.10. The question is why the repulsive volume of dendrimers is significantly smaller than that of PS?

This effect might originate in the presence of backbone oxygen atom, responsible for high macromolecular chain mobility. It is noteworthy that the PBED "segment" occupies four lattice cells not two as styrene, thus the van der Waals molar volume per lattice cell is 15.4 and 26.4 for PBED and PS, respectively. Thus, the ratio of the cell volumes, 0.58, is comparable to the quoted above ratio of repulsive cell volume, v^*(PBED)/v^*(PS) = 0.67 ± 0.10. The proposition that oxygen presence in the main chain reduces v^* was examined by plotting v^* versus ε^*, for the 52 polymers evaluated by Rodgers.[11] While for many carbon-chain macromolecules the dependence followed that for PS in Figure 6, the data points for polymers with oxygen in the main chain, e.g., polyethylene glycol (PEG), bisphenol-A polycarbonate (PC), or polyether-ether ketone (PEEK), show much lower v^*-values, falling on a dependence close to that for PBED in Figure 6. The fact that these polymers do not follow the PBED line may indicate that the latter macromolecules with one oxygen present in the backbone and another linking the terminal benzyl group have still higher flexibility.

Thus, as far as the L-J parameters are concerned, the answer to **question 2** is affirmative—the computed values of the two parameters are reasonable, considering the effect of oxygen linkage in the main and side chain.

Re Question 3

How the free volume and derivative properties change with the increasing generations?

It is normal that even if a function well describes the experimental data, the derivatives may deviate. In the present case, the S-S "equivalent" model for PBED very well describes the *PVT* surface and the first derivatives at ambient pressure. However, the experimental data for PBED deviate from the theoretical prediction for higher derivatives, e.g., for the pressure effect on κ or B. As the magnitude of the free volume fraction is the key for the liquid behavior, it is essential to know how h varies in PBED.

As stated earlier, in the S-S theory the parameters s and c define the macromolecular architecture. However, to preserve the CSP and compare the PBED with PS the "equivalent" configuration of dendritic and linear macromolecules is assumed the same: $\lim_{s\to\infty}(3c/s) = 1$, so the only distinction between PBED and PS allowed by eqs 2–4 is in the L-J parameters, v^* and ε^*. As the magnitude of the L-J attraction energy and T^* for these two polymers is similar, the main difference between them originates in the relative magnitude of v^* or V^*, reflected in the free volume quantity, h. Evidently, the free volume controls the derivatives, α and κ.

The function $h = h(P, T)$ was computed for three polymers with similar molecular mass: PS-34, G_5, and $G_{5\text{-linear}}$ at T = 345 and 395 K. For all three the isobaric h_P versus T dependence is linear:

$$h_p = h_o + h_1 T \tag{18}$$

Table 6 lists values of h_o and h_1 parameters and the correlation coefficient r at P = 20–200 MPa. The dependencies are similar, with larger pressure effect on PS-34 than that on PBE.

Figure 12 displays the computed values plotted as isothermal $h_T = h(P)$. Now the different magnitude of h and that of the P-effect on it for PBED and PS is evident. At the same T and P, the largest free volume is in G_5 and the smallest in $G_{5\text{-linear}}$. This result explains the experimental $\tilde{\kappa} = \tilde{\kappa}(\tilde{P})$ dependencies in Figure 11 where the highest value of compressibility is for the former and the lowest for the latter polymer. Furthermore, the variation of h in both PBE resins is smaller than that in PS-34. Accordingly, in Figure 11 at high P the compressibility of PBE is smaller than that of PS-34. The differences in the free volume content in these three polymers most likely originate in the nonuniform segmental density of dendrimers.[32]

In conclusion, the answer to **question 3** is also affirmative. The variability of h for PBED explains the observed difference in κ-behavior in comparison to the theoretical prediction and experimental data for linear macromolecules.

SUMMARY AND CONCLUSIONS

Application of the S-S theory to dendrimers produced excellent description of the *PVT* surface and good prediction of the first derivatives, the ambient pressure thermal expansion coefficient, α_o, and compressibility coefficient, κ_o. The ability of this simple cell-hole model to represent dendrimer behavior is remarkable. Replacement of the dendritic structure by "equivalent" linear molecule suffices for correctly predicting ambient compressibility and thermal expansion. However, the model cannot mirror the different pressure effects on the 3D dendritic macromolecules with variable (with distance from the core) segmental density, thus the computed values of the second and higher derivatives [e.g., $(\partial\kappa/\partial P)_T$] significantly deviate from the theoretical predictions and behavior of linear polymers.

The mathematical modeling of the dendrimer segmental density as a function of distance from the center of mass shows at least one maximum.[33] Consequently, if better prediction of higher derivatives is required, the S-S theory with a binary model of dendrimer molecules may be applied.

The authors express their gratitude to Michael E. Mackay (Department of Materials Science, University of Delaware, Newark, DE) for providing the tabulated *PVT* data of dendrimers. They also thank Grant Hay for his personal interest and helpful comments. After 73 years of publishing in scientific journals, this article is Robert Simha's last.

REFERENCES AND NOTES

1 Hay, G.; Mackay, M. E.; Hawker C. J. J Polym Sci Part B: Polym Phys 2001, 39, 1766–1777.

2 Hay, G. Thermodynamics and Flow Properties of Linear and Dendritic Polymer Melts, Ph.D. Thesis; The University of Queensland: St. Lucia, Australia, November 1999.

3 Fréchet, J. M. J. Science 1994, 263, 1710–1715.

4 Zoller, P.; Walsh, D. Standard Pressure-Volume-Temperature Data for Polymers; Technomic Pub. Co.: Lancaster-Basel, 1995.

5 Utracki, L. A. Polymer 2005, 46, 11548–11556.

6 Utracki, L. A. J Polym Sci Part B: Polym Phys 2007, 45, 270–285.

7 Nanda, V. S.; Simha, R.; Somcynsky, T. J Polym Sci Part C: Polym Symp 1966, 12, 277–295.

8 Simha, R.; Somcynsky, T. Macromolecules 1969, 2, 342–350.

9 Somcynsky, T.; Simha, R. J Appl Phys 1971, 42, 4545–4548.

10 Utracki, L. A.; Jamieson, A. M., Eds. Polymer Physics: From Suspensions to Nanocomposites to Beyond; John Wiley & Sons, Inc.: Hoboken, NJ, 2009.

11 Rodgers, P. A. J Appl Polym Sci 1993, 48, 1061–1080.

12 Utracki, L. A.; Simha, R. Macromol Theory Simul 2001, 10, 17–24.

13 Utracki, L. A.; Simha, R.; Garcia-Rejon, A. Macromolecules 2003, 36, 2114–2121.

14 Utracki, L. A.; Simha, R. Macromolecules 2004, 37, 10123–10133.

15 Utracki, L. A. Eur Polym J 2009, 45, 1891–1903.

16 Utracki, L. A. J Polym Sci Part B: Polym Phys 2009, 47, 299–313.

17 Utracki, L. A. J Polym Sci Part B: Polym Phys 2009, 47, 966–980.

18 Simha, R.; Wilson, P. S. Macromolecules 1973, 66, 908–914.

19 Jain, R. K.; Simha, R. Macromolecules 1989, 22, 464–468.

20 Olabisi, O.; Simha, R. J Appl Polym Sci 1977, 21, 149–163.

21 Hirschfelder, J. O.; Curtis, C. F.; Bird, R. B. Molecular Theory of Gases and Liquids; John Wiley & Sons: New York, 1954.

22 Simha, R. Macromolecules 1977, 10, 1025–1030.

23 Flory, P. J. Statistical Mechanics of Chain Molecules; Interscience Publ.: New York, 1969.

24 Moulinie, P.; Utracki, L. A. In Polymer Physics; Utracki L. A.; Jamieson A. M., Eds.; John Wiley & Sons: New York, 2009, Chapter 6.

25 Jain, R. K.; Simha, R. Macromolecules 1980, 13, 1501–1508.

26 Jain, R. K.; Simha, R. Macromolecules 1984, 17, 2663–2668.

27 Li, G.; Leung, S. N.; Hasan, M. M.; Wang, J.; Park, C. B.; Simha, R. Fluid Phase Equilib 2008, 266, 129–142.

28 Papazoglou, E.; Simha, R.; Maurer, F. H. J. Rheol Acta 1989, 28, 302–310.

29 Simha, R.; Carri, G. J Polym Sci Part B: Polym Phys 1994, 32, 2645–2651.

30 Simha, R.; Ugur, Y. J Chem Soc Faraday Trans 1995, 91, 2443–2455.

31 Van Krevelen, D. W. Properties of Polymers; Elsevier: Amsterdam, 1990, Chapter 4.

32 Cagin, T.; Wang, G.; Martin, R.; Goddard, W. A., III. In Proceedings of the Seventh Foresight Conference on Molecular Nanotechnology, Santa Clara, CA, 1999; pp 10.15–10.17.

33 Naylor, A. M.; Goddard, W. A., III; Kiefer, G. E.; Tomalia, D. A. J Am Chem Soc 1989, 111, 2339–2341.